ISSN 2447-6102

Article

A PROPULSION AND GUIDANCE SYSTEM FOR THE CONTROLLED DESCENT OF A LOW-COST CANSAT

Amani, M.R. [1,2], Díaz, M.J. [1,2], Egea, R.D. [2], Lucchese Vides, D. O. [1,2,*], Medel, R. [3], Pienizzio, A. [4], Ruiz, J.L.[2]

[1] Universidad Nacional de Tucumán - Instituto Técnico de Aguilares; profmariojadi@gmail.com
[2] Universidad Tecnológica Nacional - Facultad Regional Tucumán; dlucchese@frt.utn.edu.ar
[3] Universidad Tecnológica Nacional - Facultad Regional Córdoba; rmedel@frc.utn.edu.ar
[4] Universidad Nacional de La Plata - Instituto de Relaciones Internacionales; andrespienizzio@gmail.com
*****Correspondence: dlucchese@frt.utn.edu.ar; Tel.: +54-9-381-5302175

Received: Outubro/2025; Accepted: Novembro/2025; Published: Novembro/2025

Abstract: CanSats are non-orbital satellite models used for education under a STEM (Science, Technology, Engineering, and Mathematics) educational approach. This device promotes scientific and technological interest by providing hands-on learning in space science and technology. During CanSat contests, teams of students reproduce the process of satellite design, manufacturing, testing, launch, and operation at a small scale. Originally proposed in 1991 in the USA and Japan, the first educational use of CanSats in Argentina dates back to 2004, but only recently country-wide CanSat contests were carried out by the Ministry of Science, Technology, and Innovation (MINCYT) and the National Commission for Space Activities (CONAE). During one of these contests, a team of students and faculty from the Aguilares Technical Institute of the National University of Tucumán proposed a CanSat design to capture images of burned crop surfaces, a common environmental problem in Tucumán Province. In order to cover larger and specific areas for such recordings, the CanSat had to be controlled from the Ground Station by using a servo-controlled parawing, a 3D-printed propeller, and a two-way communications subsystem based on LoRa technology. These subsystems are rarely found at CanSat designs, and there is no bibliographic record of a design including all of the three characteristics. The team's success in coping with the complexity of the proposal resulted in them winning the "Best Technical Development" award. In this work we cover the novel design of the CanSat and its challenges, by showing the different subsystems required for achieving the primary and secondary missions.

Keywords: CanSat, Satellite, STEM Education, Communications Subsystem, Controlled Descent.

1. Introduction

Since they were first proposed in 1991, CanSat models have been widely used worldwide as a STEM (Science, Technology, Engineering, and Mathematics) teaching device. Usually in the way of extracurricular activities under the Project-Based Learning (PBL) methodology, but most notably in international, regional or national competitions [1]. These competitions challenge high-shcool- or college-level students to design and build a satellite model the size of a soda can, simulating a real aerospace mission on a small scale.

In Argentina, the National Commission for Space Activities (CONAE) and the then-Ministry of Science and Technology (MINCYT) organized two national CanSat Argentina competitions in 2022 and 2023. In these events, teams of three to five high-school students, each guided by at least one teacher, had to design and build a payload with the standard CanSat dimensions (diameter: 70 mm, height: 150 mm) to be launched on a small rocket to an altitude of approximately one kilometer [2].

A team formed by students and professors from the Aguilares Technical Institute, affiliated to the National University of Tucumán, participated in CanSat Argentina 2023 under the name of Cóndor Salvaje. The team proposed an environment-oriented Secondary Mission aimed to capture images and videos of sugarcane crops to detect fires or burned areas. In order to cover a larger area during descent, the design incorporated a propulsion system for horizontal

displacement and a ground-controlled guidance mechanism, allowing the CanSat to land near the Ground Station for safe retrieval of the unit and its collected data [3].

This work presents and validates the design of a novel low-cost CanSat that integrates a propulsion system, a guided parawing descent mechanism, and a bidirectional communication link. These elements, rarely combined in CanSat designs, enable controlled horizontal displacement and landing near the Ground Station. Thus, this paper describes the design methodology, including computational simulations and CAD modeling, the manufacturing and integration process, and experimental tests using prototypes and the final CanSat. The results demonstrate the feasibility and educational value of this approach.

2. Materials and Methods

2.1. System Design

Unlike conventional CanSat layouts, the structure was divided into two modular parts: the lower section housing electronics and the upper section integrating propulsion and guidance subsystems (Figure 1). A NoIR camera was mounted at the base with a lens opening to capture images of the surface during descent. Structural simulations using Autodesk Inventor [4] confirmed that a lightweight plastic material provided enough strength and ease of construction.

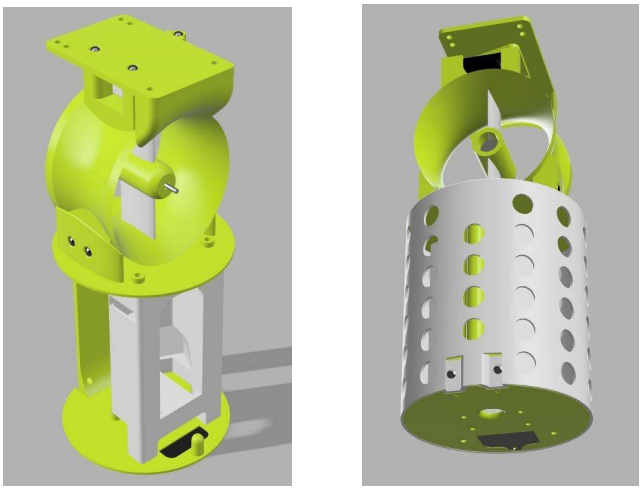

Figure 1. Design of the two-modular CanSat structure: (**a**) Interior structure; (**b**) Final assembly with exterior cover.

The overall system architecture includes the flight segment and the ground segment. The CanSat model itself represents the flight segment, while the ground segment consists of a laptop computer with a bidirectional radio link that receives telemetry and allows the operator to send control commands to the CanSat.

The CanSat was designed in compliance with the competition requirements: a maximum weight of 200 g (±10%), cylindrical geometry of 70 mm in diameter and 150 mm in height, with an additional 20 mm allowance for the parachute. The estimated release altitude was 500 m, and the maximum total cost allowed was USD 500. The mandatory primary mission consisted of recording temperature and pressure data and transmitting them to the Ground Station, while the secondary mission proposed by the team aimed to detect fires or burned areas in sugarcane fields by capturing images or videos.

The CanSat architecture comprises the five integrated subsystems shown in Figure 2. The data acquisition and processing subsystem includes temperature, pressure, gas, and GPS sensors, together with the onboard units —an ESP32 microcontroller and a Raspberry Pi Zero— responsible for control, sampling, and data storage. The propulsion subsystem employs a coreless DC motor with a ducted propeller to generate horizontal displacement. The guidance subsystem uses a Rogallo-type parawing [5] with a servomotor-driven spar rod that adjusts the lateral chords to modify wing geometry and achieve steering during descent. The communication subsystem is based on a Heltec ESP32 LoRa V2 board that transmits telemetry and receives control commands from the ground segment, where a graphical interface displays flight data in real time. Finally, the power subsystem provides energy through two LiPo batteries, one dedicated to propulsion and another to auxiliary systems.

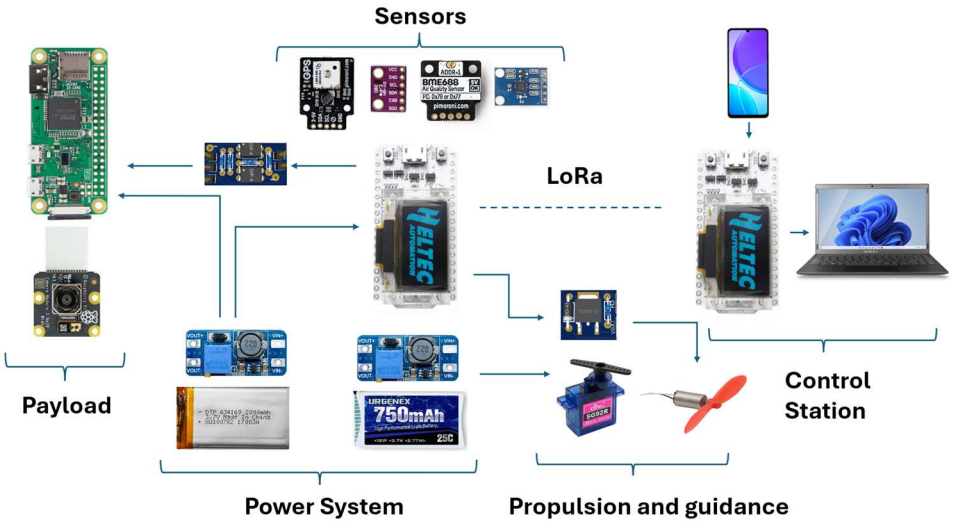

Figure 2. Layout of the CanSat subsystems: (**1**) Payload: Cameras & Sensors; (**2**) Energy: Power System; (**3**) Guidance: Propulsion & guidance; (**4**) Ground segment: Control Station; (**5**) Communication: LoRa.

Initially, a hemispherical parachute was used to reduce fall speed and ensure safe landing during tests. However, as horizontal displacement was also required, the design evolved into a paraglider, created with Single Skin software and built from fabric similar to Skytex 40. Tests showed that, although horizontal control was straightforward, the paraglider required many tensors, was complex to construct, difficult to deploy due to the large fabric area, and proved highly unstable, resulting in unsuccessful CanSat aiming.

Finally, a parawing-type speed reducer was used, based on the model proposed by American aeronautical engineer Francis Melvin Rogallo [5]. The parawing consists of a central rectangle and two side isosceles triangles, resembling a manta ray (Figure 3a). Its design considered the CanSat's weight and cylindrical shape, determining descent speed, wing geometry, anchor points, and line lengths. To determine the geometry of the Parawing, NASA Para Wing software was used (Figure 3b). This configuration achieves a terminal speed of 1–2.5 m/s in the absence of wind and allows horizontal displacement. The lateral chords can be tensioned to modify the wing's geometry and direction, enabling directional control.

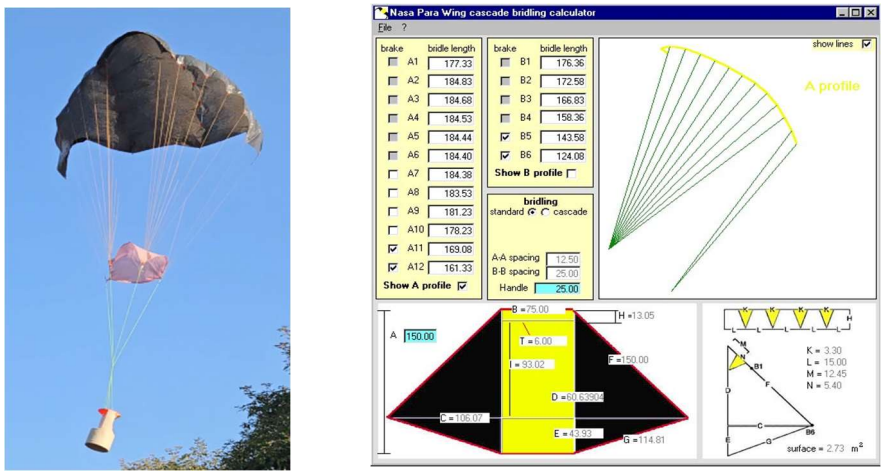

Figure 3. Parawing: (**a**) During testing; (**b**) Design by Nasa Para Wing Software.

The propulsion subsystem consists of a drone DC microengine and a two-blade propeller mounted in a duct (as shown in Figure 4) designed for maximum aerodynamic efficiency. The engine housing, attached to a vertical support, has a teardrop shape to reduce turbulence and energy loss.

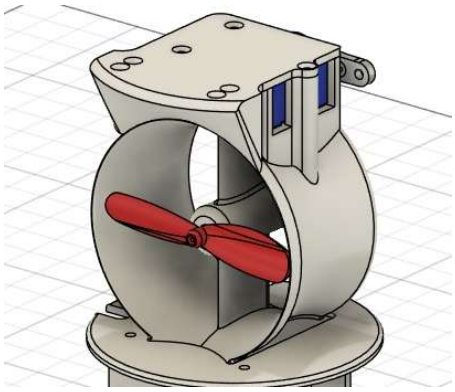

Figure 4. Propulsion subsystem.

The duct, designed in Fusion 360 [6], features a one-blade hyperboloid of revolution (Figure 5) with a major diameter of 58 mm, a minor diameter of 46 mm, a length of 37 mm, and a wall thickness of 2 mm.

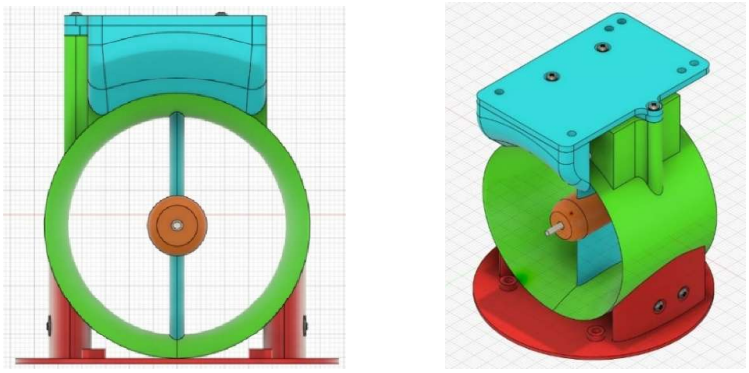

Figure 5. The designed duct.

Equation (1) defines the reference hyperbola, which revolves around the x-axis to generate the three-dimensional surface.

$$\frac{y^2}{23^2} - \frac{x^2}{24.1^2} = 1\,, \quad -18.5 \le x \le 18.5 \qquad (1)$$

The corresponding curve, plotted using Desmos, and the resulting surface generated with Surfer, are shown in Figure 6.

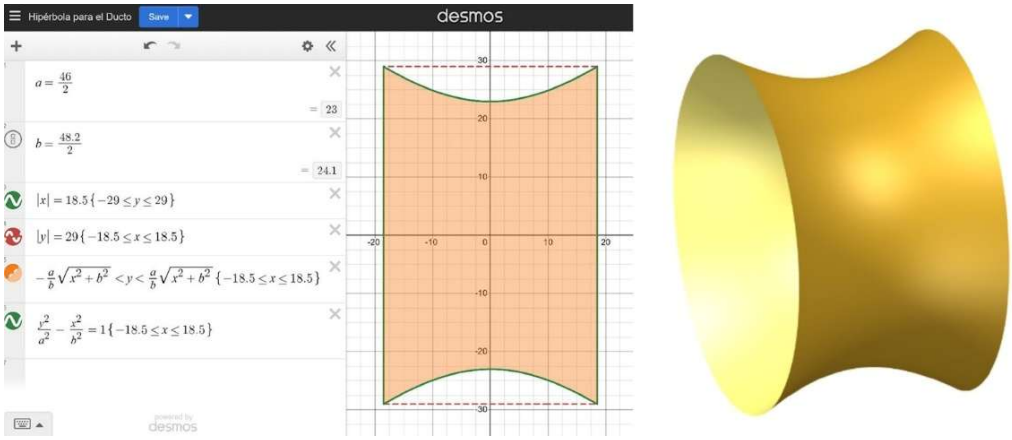

Figure 6. Surface generated using Surfer.

This geometry was selected after preliminary computational analyses demonstrated that the hyperboloid profile provides superior aerodynamic efficiency compared to cylindrical or conical ducts of equivalent dimensions. The

continuous curvature of the hyperboloid minimizes pressure gradients and turbulence intensity near the propeller's trailing region, thereby reducing flow separation and improving thrust linearity.

To further validate these advantages, a comparative CFD analysis was performed using four different duct configurations—cylindrical, conical, ellipsoidal, and hyperboloid—under identical boundary conditions. The results, summarized in Table 1, show that the hyperboloid configuration achieved the highest average exit velocity and the lowest pressure drop among all tested geometries. This combination of enhanced flow uniformity and reduced turbulence directly translates into improved thrust efficiency, confirming that the hyperboloid profile provides the most favorable aerodynamic performance for the CanSat propulsion unit.

Table 1. Comparative CFD analysis results.

Geometry Type	Major Diameter (mm)	Minor Diameter (mm)	Length (mm)	Average Exit Speed (m/s)	Pressure Drop (Pa)	Relative Thrust Efficiency (%)	Comments
Cylindrical	58	58	35	3.1	48	100 (baseline)	Simple geometry, low efficiency
Conical	58	40	37	4.2	55	118	Improved acceleration, moderated turbulence
Hyperboloid (proposed)	58	46	37	6.0	41	157	Optimal curvature, minimal wake turbulence
Ellipsoidal	58	44	36	5.2	50	135	Smooth flow, slightly higher drag near exit

The selected geometry was then analyzed in Autodesk CFD, applying an internal-flow model with a tetrahedral finite-element mesh and inlet/outlet boundary conditions. The simulation results confirmed a uniform velocity field across the exit section, with reduced wake turbulence and minimal pressure losses. A maximum propulsion velocity of approximately 0.6 m/s was obtained—about two times higher than the un-ducted configuration (Figure 7)—demonstrating the significant efficiency gain provided by the hyperboloid duct.

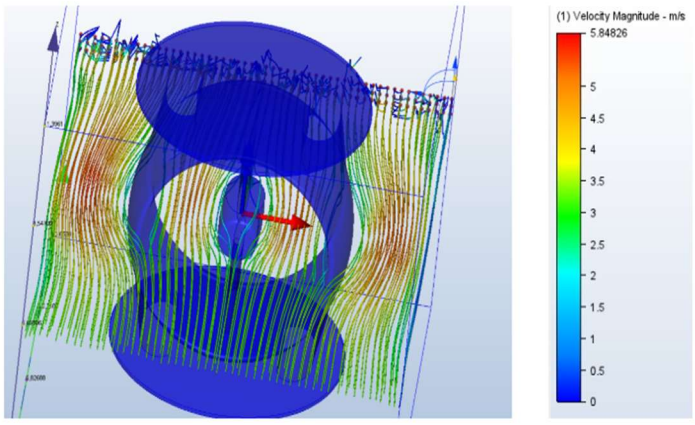

Figure 7. Computational simulations for the duct design.

The steering subsystem (Figure 8) enables guided descent by replicating the fundamental control mechanisms of a paraglider. A lightweight spar-type rod is attached to the shaft of a TowerPro SG92R digital servomotor with carbon-fiber gears and a 180° rotation range. This rod anchors two sets of Kevlar tension lines, each linked to one side of the parawing. By rotating the rod, the servomotor selectively tightens one group of lines while loosening the opposite side, producing an asymmetric change in the parawing's geometry. This differential tension alters the aerodynamic lift distribution, resulting in a controlled roll or yaw motion that allows the CanSat to change direction during descent.

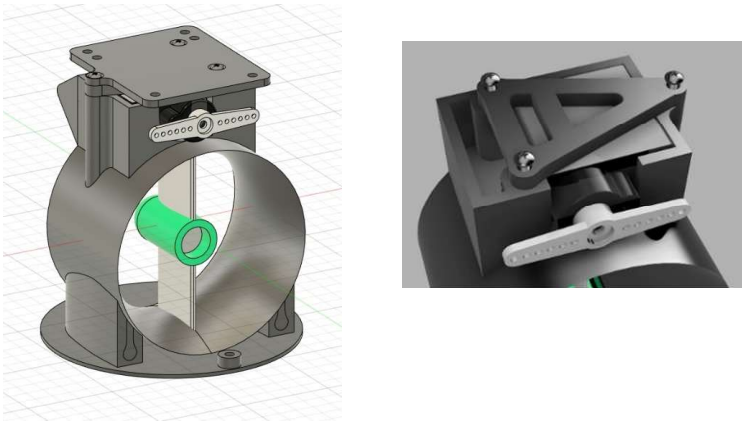

(a) (b)

Figure 8. Steering subsystem: (**a**) Mounted over the duct; (**b**) Detail of rod.

The servomotor is commanded from the Ground Station through angular setpoints transmitted over the LoRa link. These commands are processed by the onboard ESP32 microcontroller, which converts them into precise pulse-width modulation (PWM) signals to drive the steering actuator.

A Pimoroni GPS sensor was integrated to track the CanSat's position during flight. The georeferenced data is sent via the LoRa system to the Ground Station, where the operator can monitor it through the GUI and effectively control the descent, even without direct visual contact at high altitude.

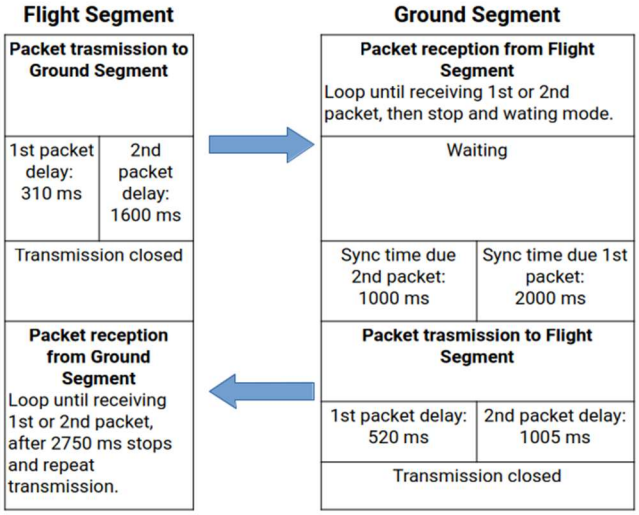

Figure 9. Communication process.

The communication subsystem was designed to transmit sensor data and video metadata from the CanSat to the Ground Station, while also enabling remote control commands to be sent back. Two Heltec ESP32 LoRa V2 boards with SX1262 transceivers were employed, providing long-range, low-power wireless communication using the LoRa protocol over unlicensed regional bands (863–928 MHz).

As the devices operate only in half-duplex mode, transmission and reception occur alternately rather than simultaneously. To ensure reliability, a redundancy scheme was implemented in which each data packet was transmitted twice and assigned a unique identifier, allowing synchronization between both LoRa nodes and reducing the impact of occasional packet loss (up to 5%) (Figure 9).

During operation, when the CanSat transmits sensor data, the Ground Station remains in a waiting loop until packet reception is confirmed. After identifying the unique code, it switches to transmission mode and sends back control

commands previously received via Bluetooth from a mobile application. The CanSat then validates the received command and resumes transmission mode, repeating this cycle throughout the mission.

The Ground Station interface was developed in Node-RED for real-time data visualization and command handling, while a simple mobile app built in MIT App Inventor provided user control via Bluetooth communication with the LoRa board.

2.2. Manufacturing

The CanSat structure was manufactured through additive manufacturing with 3D printing. Several prototypes were produced with different plastics, including PETG, polypropylene, and PLA, to evaluate strength and weight. The final model was printed entirely in PLA, which offered the best balance between mechanical resistance and low mass.

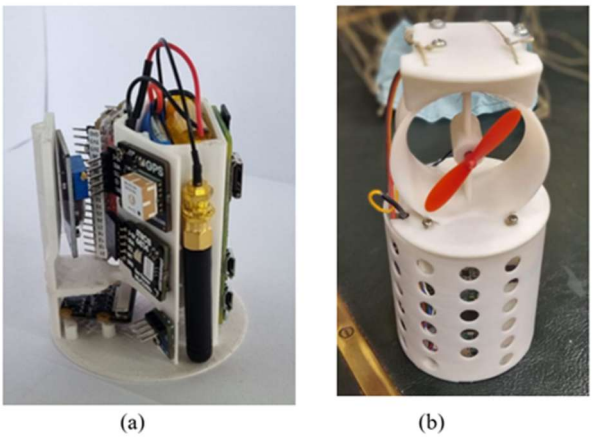

Figure 10. Integration of the CanSat components: (**a**) Internal structure; (**b**) External case.

All electronic components were assembled in the lower section of the structure (Figure 10a), while final integration is shown in Figure 10b. The design was refined until all subsystems could be accommodated within the volume and mass constraints. Two 3.7 V LiPo batteries were employed: a 1500 mAh unit for all subsystems except propulsion, and a 750 mAh high-discharge unit for the motor, meeting both energy and weight requirements. The parawing was manufactured from lightweight plastic with Kevlar thread tensors, anchored to the upper face of the structure and controlled by a 180° digital servomotor through a steering rod. Several folding methods were tested to ensure reliable deployment. For propulsion, a coreless DC micromotor with a two-blade propeller was driven by a MOSFET switch.

2.3. Testing

Several experimental procedures were designed to evaluate the performance of the CanSat subsystems prior to the final launch. To assess the descent speed reduction capability, drop tests with CanSat-equivalent masses were conducted from heights of 10 to 30 meters under wind conditions of 3–5 km/h. The descent time and stability were recorded for each trial. Deployment reliability was verified through more than one hundred parawing folding trials, performed both at ground level and from elevated platforms to ensure complete and correct deployment.

The propulsion system was evaluated by mounting the motor–propeller unit with its duct on a wheeled dynamometer setup, allowing thrust measurements to be inferred. Additional tests were carried out by suspending the CanSat model with the parawing deployed and activating the propulsion unit to observe the induced displacement.

Steering functionality was first tested by exposing the parawing to airflow generated by a high-flow fan, simulating flight conditions. The response of the steering rod–servomotor–parawing subsystem to ground-issued commands was observed. Further trials involved releasing the CanSat model from heights of 10–15 meters, as well as from a drone at different altitudes, to verify horizontal displacement under operator control, both with and without propulsion assistance.

In addition, full-scale flight tests were conducted by releasing the CanSat from a drone at various altitudes. These aimed to replicate conditions similar to those expected during the rocket launch, while ensuring safety and repeatability.

Finally, the complete system was scheduled for testing during the 2023 CanSat Argentina competition, in which the payload would be launched on a rocket to an altitude of approximately 500 m. This final trial aimed to evaluate the integrated performance of propulsion, guidance, and communication under real mission conditions.

3. Results

The experimental campaign included ground-based drop tests, propulsion trials, drone-assisted flights, and a final launch with a rocket. The results obtained in these tests are summarized below and discussed with respect to the feasibility and limitations of the proposed propulsion and guided descent system.

3.1. Ground and Drop Tests

Drop tests with equivalent masses demonstrated the descent characteristics under controlled conditions. Table 2 presents the main results, including descent time, average velocity, and horizontal displacement. These data confirmed that the parawing provided a significant reduction in terminal velocity, maintaining stability under low-wind conditions.

Initial ground tests and low-altitude drop tests were conducted to verify the mechanical stability of the CanSat and the performance of the parawing-based descent system. Using dummy payloads equivalent in mass to the flight unit, over one hundred drop trials were performed from heights ranging between 10 m and 30 m under varying wind conditions (3–8 km/h).

The deployment sequence was consistently successful, with only three partial openings recorded during early iterations, all caused by improper folding of the parawing. The final folding pattern achieved 100% deployment reliability and provided a stable descent rate between 1.07 m/s and 1.59 m/s. These values fall within the expected range predicted by the aerodynamic simulations and satisfy the competition's requirement for safe landing speed (< 5 m/s).

Video recordings confirmed negligible oscillations during descent. The stability observed in roll and pitch angles suggests that the Rogallo-type parawing configuration offers greater longitudinal stability than traditional hemispherical parachutes of equivalent projected area.

Table 2. Results of drop tests from 10–30 m.

Drop height (m)	Descent time (s)	Average speed (m/s)	Horizontal displacement (m)
10	6.30	1.59	14
20	16.5	1.21	22
30	28.0	1.07	35

3.2. Propulsion System Performance

Static and dynamic tests of the propulsion unit were performed to quantify thrust, efficiency, and energy consumption. The ducted propeller assembly was mounted on a mobile wheeled base connected to a dynamometer, allowing direct thrust measurements.

These tests confirmed the expected thrust enhancement predicted by CFD simulations. Table 3 summarizes the comparative results for different motor and propeller configurations. The results show that the duct increased propulsion efficiency while keeping current consumption within the limits imposed by the battery.

These findings demonstrate that the hyperboloid configuration enhances propulsion efficiency, validating the analytical predictions derived from the mathematical model described in Section 2.1.

Table 3. Propulsion performance under different configurations.

Motor type	Propeller type	Duct (Yes/No)	Measured thrust (N)	Current consumption (A)
Coreless DC	Two-blade	No	0.42	0.45
Coreless DC	Two-blade	Yes	0.65	0.52

3.3. Steering Tests with Drone

Drone-assisted flights were conducted at altitudes of 50, 100, and 150 m. Table 4 presents the main parameters recorded. The CanSat responded to operator commands, achieving measurable horizontal displacement, and controlled landings within the test area. Packet reception was consistently high, demonstrating the reliability of the communication system.

Telemetry data received at the Ground Station indicated stable LoRa communication throughout the tests, with packet loss remaining below 2%. The steering response time averaged 0.8 s, limited primarily by the half-duplex communication cycle of the LoRa modules.

Table 4. Results of drone-assisted tests.

Release altitude (m)	Descent time (s)	Average speed (m/s)	Landing accuracy (m)	Parawing deployment (Full/Partial/Failed)	% Packets received	Measured variables
50	49.5	1.01	7	11	Yes	100.0
100	102	0.98	10	15	Yes	99.0
150	158.5	0.95	16	21	Yes	98.5

3.4. Rocket Launch Test

The final verification was conducted during the CanSat Argentina 2023 competition. The CanSat was launched aboard a solid-fuel rocket to an altitude of approximately 500 m. Table 5 summarizes the data obtained. Although a folding issue with the rocket fairing prevented complete deployment of the parawing, the telemetry system worked as expected, and all planned mission data (temperature, pressure, and geolocation) were successfully received.

Table 5. Results of rocket launch.

Release altitude (m)	Descent time (s)	Average speed (m/s)	Landing accuracy (m)	Parawing deployment (Full/Partial/Failed)	% Packets received	Measured variables
500	80.5	6.2	67	Partial	98	Temperature, pressure, altitude, geolocation

4. Discussion

The combined experimental and computational results demonstrate the feasibility of integrating a propulsion and guidance system within the strict dimensional and weight constraints of a standard CanSat. The use of a hyperboloid duct, validated through CFD analysis and thrust measurements, represents a significant advancement in small-scale aerodynamic optimization. The improved flow uniformity and reduced turbulence confirmed that the hyperboloid profile provides superior efficiency for micropropulsion systems.

A comparison between predicted and measured thrust values shows strong correlation, with experimental results averaging 6% lower than simulated estimates. This minor discrepancy can be attributed to unmodeled frictional effects and 3D printing surface irregularities within the duct. Despite this, the measured performance demonstrates that additive manufacturing can produce aerodynamically efficient geometries suitable for real aerospace educational missions.

The steering subsystem, based on the Rogallo parawing concept, achieved both stability and directional control during descent. The lateral chord tensioning mechanism proved to be an effective way to alter wing geometry dynamically, achieving consistent horizontal displacement in response to ground-issued commands. The combined performance of the servomotor-driven actuator and propulsion unit validated the proposed guidance strategy for low-cost CanSat missions.

The LoRa-based communication system, while constrained to half-duplex operation, achieved reliable two-way telemetry and command exchange. The redundancy strategy with duplicate packets and unique identifiers ensured synchronization and data integrity. The observed latency (< 1 s) was acceptable for manual operator control and could be further optimized in future versions using adaptive timing or full-duplex alternatives.

In educational terms, the project also demonstrated the pedagogical value of integrating multidisciplinary skills—electronics, aerodynamics, programming, and systems engineering—into a single applied context. The CanSat served as a comprehensive learning platform for students, bridging theoretical knowledge with hands-on experimentation.

Future improvements will include the incorporation of inertial measurement unit (IMU) feedback for autonomous attitude control, as well as the implementation of computer vision algorithms on the Raspberry Pi Zero for autonomous landing-zone detection. These developments could expand the system's applicability to small-scale aerial platforms and remote sensing missions.

5. Conclusions

The Cóndor Salvaje team successfully designed, built, and validated a low-cost CanSat integrating propulsion, guided descent, and bidirectional communication within the constraints of a standard CanSat platform. The project confirmed the technical feasibility of achieving controlled horizontal displacement and stable telemetry using lightweight, low-power components.

The results demonstrate that compact propulsion and guidance systems can significantly expand the operational versatility of educational satellites, enabling missions that more closely replicate real aerospace challenges. This proof of concept therefore represents an important step toward more autonomous and controllable small-scale platforms.

Beyond the technological outcomes, the project served as a powerful educational framework for developing multidisciplinary competencies in students—spanning electronics, aerodynamics, programming, and systems engineering. By fostering creativity, teamwork, and experimental inquiry, this experience highlights the pedagogical potential of CanSat missions as catalysts for innovation in STEM education.

Future work will focus on extending the system's autonomy through onboard control algorithms, attitude stabilization using IMU feedback, and visual tracking for automatic landing. These improvements will contribute to advancing both the educational and research applications of low-cost micro-satellite technologies.

Funding: This work was funded by the Secretaría de Ciencia y Tecnología from the Universidad Tecnológica Nacional, Argentina, under the research project "*Development of capabilities for the design, construction and operation of nanosatellites, with a projection towards a certified CubeSat*".

Acknowledgments: The authors wish to thank the students of the Cóndor Salvaje team for their effort and dedication to design, produce, test and operate the CanSat that we show in this work.

Conflicts of Interest: The authors declare no conflict of interest.

References

1. Contente J.; Galvão C. STEM Education and Problem-Solving in Space Science: A Case Study with CanSat. Education Sciences **2022**, Volume 12(251). https://doi.org/10.3390/educsci12040251
2. CANSAT Argentina. Available online: https://www.argentina.gob.ar/ciencia/sact/cansat-argentina (accessed on 30 10 2025)
3. Amani, M.R.; Díaz, M.J.; Egea, R.D.; Lucchese Vides, D.L.; Medel, R.; Pienizzio, A. Experiencias en la implementación de un sistema de comunicación bidireccional para un CanSat dirigido desde el Segmento Terreno. Congreso Argentino de Tecnología Espacial accepted.
4. Autodesk Inventor. Available online: https://www.autodesk.com/products/inventor/overview (accessed on 30 10 2025)
5. Nasa ParaWing. Available online: http://freedom2000.free.fr/NPW_compar_profil_eng.html (accessed on 30 10 2025)
6. Fusion 360. Available online: https://www.fusion360.es/ (accessed on 30 10 2025)